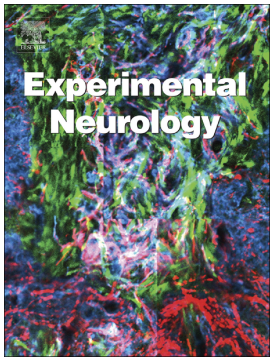

The differentiated networks related to essential tremor onset and its amplitude modulation after alcohol intake

David J. Pedrosa, Christian Nelles, Peter Brown, Lukas J. Volz, Esther A. Pelzer, Marc Tittgemeyer, John-Stuart Brittain, Lars Timmermann

PII: S0014-4886(17)30187-5
DOI: doi: 10.1016/j.expneurol.2017.07.013
Reference: YEXNR 12578

To appear in: *Experimental Neurology*

Received date: 15 May 2017
Revised date: 29 June 2017
Accepted date: 24 July 2017

Please cite this article as: David J. Pedrosa, Christian Nelles, Peter Brown, Lukas J. Volz, Esther A. Pelzer, Marc Tittgemeyer, John-Stuart Brittain, Lars Timmermann , The differentiated networks related to essential tremor onset and its amplitude modulation after alcohol intake, *Experimental Neurology* (2017), doi: 10.1016/j.expneurol.2017.07.013

The differentiated networks related to Essential tremor onset and its amplitude modulation after alcohol intake

Authors:

[1,2]David J. Pedrosa, MD; [2]Christian Nelles, MD; [1]Peter Brown, PhD; [2,4]Lukas J. Volz, MD; [3]Esther A. Pelzer, MD; [3]Marc Tittgemeyer, PhD; [1]John-Stuart Brittain*, PhD and [2,5]Lars Timmermann*, MD

[1] Nuffield Department of Clinical Neurosciences and MRC Brain Network Dynamics Unit, University of Oxford, Oxford, United Kingdom

[2] Department of Neurology, University Hospital Cologne, Cologne, Germany

[3] Max-Planck Institute for Neurological Research Cologne, Cologne, Germany

[4] SAGE Center for the Study of the Mind, University of California, Santa Barbara, USA

[5] Department of Neurology, University Hospital Marburg, Marburg, Germany

* shared senior authorship

Correspondence to:

Dr. med. David Pedrosa, Nuffield Department of Clinical Neurosciences, University of Oxford, Level 6, West Wing, John Radcliffe Hospital, OX3 9DU, The United Kingdom, Tel: +44 (0)1865 572490 email: david.pedrosa@med.uni-marburg.de

Abbreviated title: The dysregulated networks of Essential tremor

Target-Journal	**Word count**	**References:**
Experimental Neurology	Abstract: 226; Manuscript: 5140; Figures: 5; Table: 1	60

Abstract

The dysregulation of endogenous rhythms within brain networks have been implicated in a broad range of motor and non-motor pathologies. Essential tremor (ET), classically the purview of a single aberrant pacemaker, has recently become associated with network-level dysfunction across multiple brain regions. Specifically, it has been suggested that motor cortex constitutes an important node in a tremor-generating network involving the cerebellum. Yet the mechanisms by which these regions relate to tremor remain a matter of considerable debate. We sought to discriminate the contributions of cerebral and cerebellar dysregulation by combining high-density electroencephalography with subject-specific structural MRI. For that, we contrasted ET with voluntary (mimicked) tremor before and after ingestion of alcohol to regulate the tremorgenic networks. Our results demonstrate distinct loci of cortical tremor coherence, most pronounced over the sensorimotor cortices in healthy controls, but more frontal motor areas in ET-patients consistent with a heightened involvement of the supplementary motor area. We further demonstrate that the reduction in tremor amplitude associated with alcohol intake is reflected in altered cerebellar – but not cerebral – coupling with movement. Taken together, these findings implicate tremor emergence as principally associated with increases in activity within frontal motor regions, whereas modulation of the amplitude of established tremor relates to changes in cerebellar activity. These findings progress a mechanistic understanding of ET and implicate network-level vulnerabilities in the rhythmic nature of communication throughout the brain.

Key words:

Essential tremor, Beamformer, DICS, MRI

Abbreviations

BEM – Boundary element method

CI – Confidence interval

CSD – Cross-spectral density

DBS – Deep Brain Stimulation

DICS – Dynamic imaging of coherent sources

DPSS – Discrete prolate spheroidal sequences

EDC – *Musculus extensor digitorum communis*

EMG – Electromyography

ET – Essential tremor

FoV – Field of view

M1 – Primary motor cortex

MDEFT 3D – Modified driven equilibrium Fourier Transform in 3D

MEG – Magnetoencephalography

PCA – Principal component analysis

RMS – Root mean square

ROI – Region of interest

SMA – Supplementary motor area

TE – Echo time

TI – Inversion time

TR – Repetition time

VLp – Posterior part of the ventrolateral thalamus

Introduction

Tremor manifests as a common symptom in a diverse range of movement disorders and can be a devastating burden on everyday life. Essential tremor (ET) is the most commonly encountered entity, in which patients develop postural and/or intentional tremor predominantly of the upper extremities, although other parts of the body may also be affected. Despite the high prevalence of ET its pathomechanisms remain largely unknown.

Like many tremor syndromes, early studies posited a single oscillator hypothesis – that one brain region accounts for tremulous outflow. This notion has been displaced in favour of disruption in a more widespread 'tremor network' comprising multiple brain regions (for a review see Raethjen and Deuschl, 2012). In this context, hypersynchronisation of the cerebello-thalamocortical pathways has become a prime focus of research for several reasons. Firstly, abundant behavioural and imaging studies implicate cerebellar disturbances in ET (Bhalsing et al., 2013; Jenkins et al., 1993; Popa et al., 2013; Wills et al., 1994). Secondly, tremor relief by medication (Boecker et al., 2010) – or reduction in tremor after alcohol intake – closely relate to changes in cerebellar activation (Boecker et al., 1996). Finally, medically refractory tremor may be treated by inducing functional or structural thalamic lesions, most likely targeting abundant cerebellar input to and dense cortical projections from the posterior parts of the ventrolateral thalamus (VLp, Kelly and Strick, 2003; Middleton and Strick, 2001).

Intraoperative recordings during deep brain stimulation (DBS) electrode implantation within the VLp, or electrophysiological studies during the days thereafter have begun to shed light on the underlying pathophysiology of ET, yet are at the same time hampered by our lack of knowledge about the functional organisation of thalamocortical pathways underlying normal motor function. Thus, it has been demonstrated that oscillatory tremor activity has a topographic representation in the VLp (Pedrosa et al., 2012), that relies heavily on sensory feedback (Pedrosa et al., 2014; Schnitzler et al., 2009). Moreover, electrical pulses delivered to

the VLp may disrupt tremor when delivered both at high frequencies (Benabid et al., 1991) and at lower frequencies when locked to certain phases of tremor oscillations (Cagnan et al., 2013, Cagnan et al. 2016). The most effective thalamic targets for interventions remain the cerebellar-recipient zones, emphasising the critical nature of this node.

More recently, however, considerable literature has developed around cerebral involvement in ET. Specifically, cortical motor areas appear to be involved in the tremulous drive to muscles (Govindan et al., 2006; Hellwig et al., 2001). In addition, magnetoencephalographic (MEG) results and studies applying combined EEG and local-field potential recordings revealed tremor-related synchronisation between cortical motor areas, the thalamus and the cerebellum (Marsden et al., 2000; Muthuraman et al., 2012; Schnitzler et al., 2009). Current theories on ET pathomechanisms implicate both cerebellar and cerebral motor regions (Buijink et al., 2015; Neely et al., 2015). Specifically, there is an emerging notion that dysregulation in cerebellar outflow to cerebral cortex results in compensation by SMA that mitigates tremulous activity (Gallea et al., 2015). When actively engaged, such as during motor tasks, the compensatory role of the SMA breaks down leading to peripheral tremor.

The above observations suggest at least two key nodes of interest in the generation and modulation of essential tremor; the cerebellum and the SMA. Tremor-related SMA activity has been hypothesised to be primarily compensatory. As such it should be absent when healthy subjects voluntarily mimic tremor. In contrast, the response of VLp interventions suggests that the cerebellum and its outflow may be involved in more directly promoting tremor. As such, we predict a relationship between tremor-related cerebellar activity and manipulations of tremor amplitude. To test these predictions we studied the functional connectivity of cerebral and cerebellar regions with tremor output using high-density EEG (HD-EEG) in cohorts of ET-patients and age- and gender-matched healthy control subjects and manipulated tremor amplitude through alcohol intake.

Methods

The study was approved by the local Ethics committee and carried out in accordance with the Declaration of Helsinki. All patients had given their written informed consent prior to participating.

Patients and clinical evaluation

For this pre-post study, 20 right-handed patients suffering from ET according to the diagnostic criteria of the Consensus statement of the Movement Disorder Society Group (Deuschl et al., 1998) were investigated. Three ET-patients were characterised as mixed-handed by the Edinburgh handedness inventory (EHI scores < 50) and were replaced by three further right-handed ET-patients. Twenty right-handed, gender- and age-matched healthy volunteers served as control group. To rule out a significant level of cognitive impairment, participants underwent a dementia screening test (DemTect) with cut-off below 12 (Kalbe et al., 2004). Response times were evaluated in a simple task in which subjects were instructed to press a button following a visual cue.

No control subject was under medication potentially influencing the central nervous system, but two ET-patients took primidone and two more received propranolol. These patients were asked to discontinue their medication at least 24 hours in advance of the study. All other patients were untreated. For more details on ET-patients, cf. Supplementary data.

Electrophysiological recordings

Participants were seated in a reclining armchair with neck and back supported and EEGs were recorded using an elastic cap with 128 electrodes mounted in a spherical array (Easy-Cap GmbH, Herrsching, Germany). To maintain electrode impedances below 10 kΩ, conduction gel was applied. The used caps were standardized and placed according to the 10/10 system.

Individual electrode locations thus resulted from interpolation from the individual 3T MRI scans and given fiducial points (see below). The relationship between electrodes and MRI was inspected visually for every subject. Additionally, activity of the *Musculus extensor digitorum communis* (EDC) of the right forearm was recorded using surface electromyography (EMG) electrodes while a tri-axial accelerometer placed on the centre of the right wrist registered tremulous arm activity. All data were recorded on a BrainAmp® standard amplifier (Brain Products GmbH, Gilching, Germany), low-pass filtered at 1 kHz and digitized at a sampling rate of 5 kHz. The EMG of the EDC of an ET-patient is illustrated in Figure 2.

Motor paradigm

The motor paradigm consisted of two conditions: i) a resting state (baseline) in which participants were asked to remain in a relaxed position with their arm supported and ii) voluntary elevation of the right forearm by about 10-15 cm above the arm of an armchair with an extended wrist and extended fingers for 3.5 secs while their elbow remained on the arm of the chair. These short periods of postural contraction were selected to focus on neurophysiological changes underpinning the onset of sustained tremor and to avoid fatigue which may have occurred during longer trials. Our task elicited involuntary tremor in ET-patients, whereas control subjects were instructed via video to perform rhythmic movements of the forearm and wrist to mimic tremor. Both tasks were thoroughly explained in advance of the experiments and all participants received the opportunity to practise them. The sequence of conditions was randomised with an unequal allocation ratio of 2:1 (tremor vs. rest conditions). Participants were instructed to fixate the centre of a computer screen during the experiment and to avoid excessive swallowing or blinking during the tasks. Every trial consisted of a task instruction displayed for 5 secs, followed by a red fixation cross (foreperiod; randomised duration between 1.3-4.8 secs), then a green cross for the duration of the trial (3.5 secs). At the end of the trial the red cross reappeared for 2.5 secs (see Figure 1). Each task was repeated 18 (rest condition) and 36 times (tremor).

To analyse modulation of tremor, after the completion of the first experiment all participants were asked to consume 1.5 alcohol units (one bottle of 330 ml, 4.8 Vol. % "Kölsch", i.e. local lager beer) and the experiment was repeated 30 minutes after alcohol intake.

Magnetic resonance imaging data acquisition and image pre-processing

Structural MR images were acquired using a 3T Siemens Trio Scanner (Siemens Healthcare, Erlangen, Germany). A structural data set was recorded with a twelve channel array head coil using a whole brain field of view (FoV) and with the following configuration: MDEFT-3D (T1-weighted, TR = 1930 ms, TI = 650 ms, TE = 5.8 ms, image dimension = 256 x 256 x 128, sagittal slices with a resolution of 1 x 1 x 1.25 mm^3, flip angle 18°). One ET-patient declined to undergo an MRI scan citing claustrophobia.

Data pre-processing

All data pre-processing was carried out on a personal computer using SPM12 (see http://www.fil.ion.ucl.ac.uk/spm/) and the Fieldtrip toolbox for EEG/MEG-analysis (Donders Institute for Brain, Cognition and Behaviour, Radboud University Nijmegen, the Netherlands, see http://www.ru.nl/neuroimaging/fieldtrip). Pre-processing of the EMG corresponded with standard routines, i.e. notch filtering the line noise, high-pass filtering (30 Hz), then full-wave rectification and low-pass filtering at 50 Hz with both filters using a 3rd order Butterworth filter (Negro et al., 2015). EEG and accelerometer data were high- and low-pass filtered applying separate zero-phase (forward-backward), 3rd order Butterworth filters with 0.5 Hz and 48 Hz cut-off frequencies, respectively.

EEG artifacts were detected and discarded as follows: First, independent component analysis was performed (Delorme et al., 2007) and blink artifacts identified by visual examination were removed. Second, EEG channels were classified as poor, when their mean amplitudes were either smaller than 0.07 μV or exceeded 120 μV. In these cases, electrode channels were

removed and interpolated using spherical splines (Perrin et al., 1989). For that, the fieldtrip default was used, that is channels within 4 cm distance were used to interpolate the rejected channels. All electrophysiological data (EEG, accelerometer and EMG) were downsampled to 100 Hz and epoched from +1.5 secs. to +3.5 secs (i.e. resulting in trials of 2 secs duration) relative to onset of the green visual cue to ensure movement transients were avoided. Trials in which participants performed the wrong task (e.g. lifted the arm during a resting condition) were discarded.

In a final step, the default electrode positions delivered by the manufacturer (Easy-Cap GmbH , Herrsching, Germany) were co-registered to the individual T1-weighted and MNI-aligned MRI image. Co-registration relied on three fiducial points: a) nasion b) left and c) right pre-auricular points**.** In the single case of a missing structural MRI, the standard template brain implemented in SPM12 was used. Thus, at the end of pre-processing all EEG and MRI data were converted to the same coordinate system to ensure compatibility.

Tremor analyses

Tremor severity was estimated for trials before and after alcohol ingestion using the root mean square (RMS) of the processed EMG. Due to higher signal-to-noise ratios, tremor frequency was assessed from the tri-axial accelerometer recordings rather than EMG. For this purpose, principle component analyses (PCA) were performed and the first principle component was extracted for further analysis. Individual tremor frequencies were identified in the respective power spectra.

Spectral analyses

Power spectra and cross-spectra were computed using Thomson's multitaper method (Mitra and Pesaran, 1999; Thomson, 1982). We denote the cross-spectrum between two signals x and y as S_{xy} with individual power spectra (S_{xx} and S_{yy}) analogously defined. Two tapers per trial

were applied resulting in 1 Hz spectral smoothing. Coherence between the pre-processed EMG signal and each EEG sensor resulted from

$$Coh = \frac{|\langle S_{xy}\rangle|^2}{\langle S_{xx}\rangle \cdot \langle S_{yy}\rangle} \quad (1)$$

where $\langle\cdot\rangle$ indicates averaging across trials. Throughout this manuscript coherence describes phase and amplitude coupling of either cerebellar or cerebral activity with the EMG which does not necessarily imply a direct dependence or drive. Power estimates were log-transformed and coherence values were normalised to z-scores in order to reduce variance across subjects and to identify local regions of peak coupling.

Sensor level analyses

We considered two conditions for our statistical analyses: 1) rest/baseline condition and 2) tremor condition, i.e. mimicked tremor for control subjects or postural tremor for ET-patients. The use of two conditions is important especially at deeper brain structures, where lower signal-to-noise ratios may result in spurious coherence values (Groß et al., 2001). Subtracting two conditions minimises this bias. However, to account for unequal numbers of trials between rest and tremor conditions we first needed to z-transform coherence values per task in accordance with Bokil et al. (2007):

$$Z_{coh} = \frac{tanh^{-1}(Coh_{cond}) - \left(\frac{1}{(df-2)}\right)}{\sqrt{\frac{1}{(df-2)}}} \quad (2)$$

with Coh_{cond} representing coherence values for the respective condition, $tanh^{-1}$ the inverse hyperbolic tangent and df the degrees of freedom in that condition. The latter resulted from the number of tapers applied and the number of trials available.

Coherence differences between tremor and rest conditions at sensor level were analysed using nonparametric, cluster-based permutation statistics to control for multiple comparisons (Maris, 2012; Maris and Oostenveld, 2007). This procedure comprised three steps: first, paired-sample *t*-tests were drawn between conditions. Second, clusters of adjacent data points (i.e. sensors adjacent in space) were defined using the maximum of summed *t*-statistics at a threshold of $p < .01$. Finally, these clusters were evaluated against a reference distribution which was obtained by randomly shuffling conditions within participants 50,000 times (Maris and Oostenveld, 2007).

Given the nature of the two conditions, higher power during tremor has to be expected which may itself cause differences in coherence. To counteract the effects of power on our results, we additionally tested postural tremor against randomly permuted tremor activity. To do so, the trial sequence for the (tremulous) EMG within a participant was randomly shuffled 500 times while leaving EEG channels unchanged and the resulting cross-spectra were averaged. This procedure compares the original (unshuffled) data against a surrogate that preserves the same level of power in the EEG and the EMG, but dissociated temporal coupling. Statistical testing again corresponded to nonparametric, cluster-based permutation statistics using paired-sample *t*-tests between the real and the shuffled data with clusters being defined on maximum of summed *t*-statistics.

Source reconstruction

In the past two decades the capacity to spatially filter EEG data (i.e. beamforming) has greatly improved its inferential power. Applying such techniques, the neural source of oscillatory activity may be unveiled whilst circumventing volume conduction issues (for review see Schoffelen and Gross, 2009). We employed the Dynamic Imaging of Coherent Sources (DICS) beamformer (Groß et al., 2001). This technique has been repeatedly used to detect cerebral but also cerebellar coupling (Groß et al., 2001; Muthuraman et al., 2012; Schnitzler et al., 2009) and

was particularly appealing given our interest in a narrow signal band around 3-10 Hz (i.e. the tremor frequency). For that purpose, we first imposed a standard 8 mm^3 grid covering the entire brain (Groß et al., 2001). This grid was spatially normalised based on individual anatomy resulting in grid points with comparable anatomical locations across subjects. The acquired structural MRIs were used to construct individual volume conduction models, based on the boundary element method (BEM) (Phillips, 2000, Hamalainen and Sarvas, 1989). This facilitated a view on how dipole sources at each grid point would project to the sensors. A 'common spatial filter' was applied across both task conditions. That is, all available trials (rest and tremor conditions) contributed to the computation of the cross-spectral density (CSD) matrix before individual trial data were projected through this filter. This was intended to prevent bias toward either condition. Data were Fourier transformed analogous to sensor level analysis using two tapers resulting in a 1 Hz spectral smoothing. To offset rank deficiency, the resulting cross-spectral density (CSD) matrix was regularised prior to matrix inversion by adding 10 % of the average sensor power to the main diagonal (Craddock et al., 2015). Finally, power was extracted for each voxel (in the MNI grid) and corresponding coherence with the EMG signal was computed using the first principal component, that is, the dipole orientation maximising signal power.

Statistical interferences of source level data

In a similar vein to the sensor level analysis, we first *z*-transformed the estimates of source level coherence (Equation 2). To circumvent a multiple-comparisons explosion we combined our sensor-space analysis results with the results from the averaged raw coherence values (see Figure 2) and *a priori* hypotheses about the brain regions related to tremor, and thus restricted source space analysis to broad bilateral cerebral and cerebellar regions based on the literature described in the introduction. Specifically, we restricted our analysis to those domains spanning Brodmann Areas 1-4 and 6 as well as the bilateral cerebellum. As we used standardised dipole locations, regions of interest (ROI) could be defined according to available atlases: for

Brodmann Areas 1-4 and 6 and Cerebellum the SPM Anatomy Toolbox (Eickhoff et al., 2005) and additionally the Automated Anatomic Labeling, (AAL, Tzourio-Mazoyer et al., 2002) for the Supplementary Motor Area (SMA). Although other deep brain regions such as the thalamus may contribute significantly to tremor, we limited our analyses to superficial structures due to the loss of signal power and spatial selectivity at deeper sites (see Figure 2). The resulting de-biased coherence estimates for every voxel in the preselected ROI were tested for exchangeability of conditions with a two-tailed cluster-based permutation paired t-test (50,000 permutations, voxel cluster-inclusion criterion: $p < .01$, nonparametric on individual voxels, with maximal summed t-values of neighbouring voxels as cluster statistics). This approach permits further spatial inference (e.g. laterality) within the restricted ROI domains. For the interpretation of coherence results, we additionally tested for differences between true coherence and coherence with permuted EMG (for details see description in sensor level analyses) again with a two-tailed, cluster-based dependent samples t-test (50,000 permutations, voxel cluster-inclusion criterion: $p < .01$, nonparametric on individual voxels, with maximal summed t-values of neighbouring voxels as cluster statistics). Furthermore, to examine differences in locations of peak coherence between groups, we computed Hotelling's T-squared statistic and its chi-squared approximation (Hotelling, 1931) using the individual locations of maximum coherence.

In a final step, we analysed the relationship between power and coherence changes and alcohol effects on RMS of the EMG. For this purpose t-statistics of regression coefficients for every voxel within the ROI were tested with a two-tailed cluster-based permutation tests across participants (50,000 permutations, cluster-inclusion criterion: $p < .05$, nonparametric on individual voxels, with maximal summed t-values of neighbouring voxels as cluster statistics). Moreover, individual power and coherence values at locations with strongest difference between rest and tremor values (that is, SMA for ET-patients and M1 for control subjects) were extracted for each individual for the without alcohol and with alcohol conditions. This difference

was related to changes in tremor amplitude due to alcohol in ET-patients and control subjects using Spearman's rank correlation.

Results

Clinical data and accelerometer recordings

In total, five subjects had to be excluded from the study: One patient exhibited considerable rest tremor in the baseline condition, two control subjects and one ET-patient showed artifacts in more than 40 % of the EEG channels while one ET-patient was excluded due to more than 50 % 'wrong trials' (see above). This left 18 healthy control subjects (age 48.6 ± 17.9 years (average ± S.D), 10 female) and 17 ET-patients (aged: 51.1 ± 14.5, 8 female). Patients suffered from tremor for 26.2 ± 15.3 years. No significant group differences were observed for age, educational years, response times or total DemTect scores (all $p > .1$). In the control group, RMS of the mimicked tremor signal significantly increased after alcohol intake (43.0 μV^2 versus 36.0 μV^2, $z = 2.20$, $p = .028$) whereas ET-patients showed a significant decrease of tremor amplitude (15.2 μV^2 versus 16.9 μV^2, $z = -2.11$, $p = .035$). The latter results are summarised in Figure 2, while further participant information is available in Table 1.

Sensor level analyses

Artifact-free data were available from 16.2 ± 3.5 (average ± S.D.) trials of 2 secs duration per subject for the rest conditions and 27.7 ± 6.2 trials per subject for tremor conditions. Permutation tests of ET-patients' and healthy control subjects' coherence rendered highly significant differences between the postural tremor and rest conditions in both groups (both $p < .01$). Cluster-based corrections for multiple comparisons revealed clusters in the contralateral sensorimotor area in healthy controls with the cluster for ET-patients appearing more medially as illustrated in Figure 3a and 3b. Results were similar for the comparison of coherence during postural tremor with coherence in the same data but with the order of EMG trials shuffled (see Methods). In addition, z-transformed coherence differences between the

conditions at EEG sensors close to the contralateral (left) sensorimotor cortex showed frequency specificity for the tremor frequency as illustrated in Figure 3c. Note that this frequency selectivity was unlikely to arise from tremor related movement artefact at the EEG level, as coherence was focal and maximal over the contralateral hemisphere.

Localization of coherent sources

We estimated cerebral and cerebellar coherence with EMG from a source grid restricted to the regions of interest expected to be involved in the generation of mimicked tremor and essential tremor (cerebral cortex and cerebellar regions). There were significant differences between the postural tremor and rest conditions in both the control and patient groups (both $p < .01$, cluster-corrected). Comparable to the results obtained at the sensor level, the spatial distribution of clusters differed between groups (see Figure 4). Movement-induced differences were localised in the left cerebral hemisphere with a peak at -44, -28, 60 [MNI coordinates] in control subjects ($p < .01$). For ET-patients, coherence differences peaked closer to midline structures at -20, -20, 68 [MNI coordinates]. These cluster results survived permutation testing (both $p < .01$) and were centred about distinct locations in the ET compared with the control group (Hotelling's T^2, $\chi^2 = 9.8$, $df = 31$, $p < .05$; individual peak coherence locations are illustrated in Figure 4c). Similar results were observed when comparing postural tremor with postural tremor using shuffled EMG ($p < .01$ for both groups), demonstrating that the result corresponds to a difference in coupling dynamics rather than an inherent difference in power between tremor and rest conditions.

Effect of alcohol

Finally, we examined the relationship between changes in coherence with changes in tremor amplitude due to alcohol ingestion. No difference in coherence occurred following alcohol, suggesting variation in changes across patients. This motivated us to explore whether some of this variance could be ascribed to differences in tremor attenuation following alcohol ingestion.

Regression analysis (change in peripheral tremor amplitude due to alcohol intake against change in coherence) for ET-patients showed a significant positive relationship located in and limited to the cerebellum with a local maximum at -28 -84 -36 [MNI coordinates, $F_{1,15}$ = 9.37, ρ = .38, p = .008; see Figure 5). There was no significant relationship for control subjects. There were no significant relationships between tremor amplitude and source power or coherence in the identified cortical clusters in SMA (ET-patients) or M1 (control subjects) after alcohol intake (all p > .05).

Discussion

The notion that ET can be considered the purview of a single aberrant oscillator appears over-simplistic. Instead, converging lines of evidence point towards a network-level mechanism in which dysregulation across cerebellar and cerebral regions leads to a gated outflow through the broader cerebellar-thalamo-cortical circuit (Brittain and Brown, 2013; Raethjen and Deuschl, 2012). But how this manifests and to what extent the various elements in this pathway contribute remains a matter of considerable debate. Here, we demonstrate similar, yet subtly distinct representations of corticomuscular coherence in ET-patients compared with mimicked tremor in healthy control subjects. Furthermore, we dissociate cerebral from cerebellar modulation of, or by, tremor. Cerebral sensorimotor regions dominate coherence between brain and muscle when contrasting tremulous with resting (baseline) conditions, whereas cerebellar regions are implicated in the amplitude modulation of tremor following alcohol ingestion, as evinced by the relationship between changes in coherence between brain and muscle with those in tremor amplitude following alcohol intake.

Imaging studies have fundamentally shaped our understanding of the brain regions involved in the pathophysiology of ET, broadening its origin to widespread alterations in brain activity. There is now abundant imaging and clinical evidence implicating a disruption of cerebellar activity in ET (for review, see Cerasa and Quattrone, 2016). Indeed, a relationship between tremor amplitude and bilateral cerebellar activation has been demonstrated (Boecker et al., 1996) and – more generally – correlations between tremor severity and cerebellothalamic connectivity (Buijink et al., 2015). Nevertheless, recent functional imaging results equally highlight SMA grey matter increases in ET (Gallea et al., 2015) and augmented SMA activation compared to healthy control subjects (Neely et al., 2015), thus raising the question how functional alterations in cerebellar and cortical activity interact to give rise to tremor in ET.

Despite the inherent spatial limitations incumbent with conventional EEG studies, a growing body of evidence highlights the importance of cortical motor regions in ET pathophysiology (Govindan et al., 2006; Hellwig et al., 2001). Notably, some authors have highlighted that coherence is not necessarily restricted to primary motor areas, but appears more medial and frontal as well (Muthuraman et al., 2012; Raethjen et al., 2007; Schnitzler et al., 2009). Our results concur with these findings yet additionally demonstrate that peak activations in ET and control subjects – while topographically similar – are in fact subtly distinct.

A different question is whether the SMA directly modulates tremor or rather acts through other regions, e.g. the primary motor cortex. Brain imaging results may render some indirect indications here. Grey matter increases have been observed in the SMA of ET-patients along with enhanced structural connectivity between SMA and corticospinal tracts (Gallea et al., 2015). In light of decreased connectivity between primary and secondary motor cortices in ET (Neely et al., 2015), one may speculate that the SMA may fulfil a compensatory role, i.e. reduce tremor induced at subcortical levels. Interestingly, we failed to demonstrate modulation of coherence between SMA and muscles after alcohol intake (resulting in decreased tremor), which might be expected of a compensatory mechanism. In contrast, support for a more direct and specific involvement of the SMA in ET generation stems from non-invasive brain stimulation. Whereas TMS over motor areas including the SMA leaves tremor amplitude unchanged (Hellriegel et al., 2012), a delay on tremor bursts (i.e. a tremor reset after TMS pulses) was noticed specifically after TMS of the SMA (Lu et al., 2015). Results from TMS studies further support our secondary finding that alcohol intake – which reduced tremor amplitude in ET-patients – positively correlated with cerebellar activity, yet not cerebral activity. Hence, inhibitory transcranial cerebellar stimulation in ET entails prolonged tremor amplitude attenuation (Gironell et al., 2002; Popa et al., 2013). A reset of tremor similar to the one encountered with SMA stimulation was, in contrast, not observed after cerebellar stimulation (Lu et al., 2015; Pinto et al., 2003).

Notably, the idea of diverging mechanisms for distinct aspects of tremor has been put forward for other tremor entities in the past. In tremulous Parkinson's disease (PD), basal ganglia dysfunction has been related to tremor emergence whereas cerebellar activation was associated with tremor amplitude modulations (Helmich et al., 2011). Although the comparison is somehow flawed given the rapid changes in amplitude and frequency in PD compared to ET which manifests rather steadily at one frequency (Brittain et al., 2015), it may, nevertheless, raise the intriguing hypothesis that different tremor syndromes share common substrates. Indeed, disruption at various levels within the cerebello-thalamocortical pathway, or the cortico-basal-thalamo-cortical pathway, which are inherently intertwined to regulate movement, may be able to drive these circuits into aberrant, tremor generating neural activity.

In support of the above hypothesis of network dysfunction across a common tremor network ablative treatments targeting the ventrolateral thalamus produce remarkable tremor amplitude reduction across a range of tremor aetiologies (Taha et al., 1999). Both mathematical models (McIntyre et al., 2004a; McIntyre et al., 2004b) and functional imaging studies indicate activation of thalamic projections to cortical motor areas in ET (Ceballos-Baumann et al., 2001; Gibson et al., 2016; Haslinger et al., 2003) and specifically SMA activation (Perlmutter et al., 2002) by successful thalamic DBS, consistent with theories that suggest DBS supresses or filters pathologically synchronised oscillatory activity. The remarkable role of both cerebellum and SMA is further emphasized by the fact that the most efficacious results achieved with DBS are attained with electrodes implanted in the vicinity of tracts originating in deep cerebellar nuclei and projecting via the thalamus to motor areas (Klein et al., 2012). Indeed, a recent study investigating the effects of thalamic stimulation with functional MRI found that the strongest decrease in activation following thalamic DBS was in the contralateral cerebellum and sensorimotor cortex (Gibson et al., 2016).

We observed a robust relationship between cerebellar coherence and change in tremor amplitude following alcohol in-take that peaked contralaterally. Although this might seem

contradictory at first glance, bilateral activations in ET have been reported (Broersma et al., 2016) and, more importantly, contralateral cerebellar activations have been related to both changes following alcohol in-take (Boecker et al., 1996) and the effectiveness of Deep Brain Stimulation (Gibson et al., 2016). Several potential post-hoc explanations can be proposed, but perhaps the most parsimonious is that cerebellar influence over tremor is not exclusively unilateral, but that the more pronounced tremor activity affecting the ipsilateral cerebellar hemisphere limits its functional response to alcohol.

Some limitations of our study require further attention. Although increasingly prevalent in the literature (Groß et al., 2001; Muthuraman et al., 2014; Muthuraman et al., 2012; Schnitzler et al., 2009), the spatial filtering of sources from the cerebellum remains contentious due to a lack of a verified forward model of cerebellar emissions. In particular in our study, the reported lack of change in coherent cerebellar activity between rest (baseline) and tremor conditions may have been due to the reduced signal quality available from cerebellar regions, but also due to physiological variation between subjects. Some of this variance may relate to differences in the response to alcohol, as evinced by the significant positive relationship between changes in cerebellar activity and changes in tremor amplitude due to alcohol intake (a result that was specific to cerebellar – as opposed to cerebral – regions).

The spatial resolution of our findings, particularly those in the cerebellum, is also limited, and this may also be relevant with respect to the aforementioned contralateral peak in correlation between changes in cerebellar activity and changes in tremor amplitude due to alcohol intake. Accordingly, unthresholded *t*-statistics are presented in all diagrams so that the relative contribution of different cerebellum/cerebral cortical areas can be assessed. However, it could be argued that the dense foliations of the cerebellar cortex may actually be paradoxically conducive to an EEG/MEG signal (indeed, some of the earliest MEG literature concerned the *in vitro* turtle cerebellum- see Okada et al., 1987), and subject specific head models were implemented to optimise lead-field calculations.

Another limitation is that by restricting analysis to cortical and cerebellar parts of the 'tremor network' no statement is possible in terms of the role of other subcortical areas. Further work is required to establish the role of e.g. the thalamus or the inferior olivary nucleus during tremor generation and its modulation. Besides, all participants in this study were relatively young in age while there is an increasing literature around possible early and late forms of ET (Deuschl et al., 2015). We therefore cannot rule out the possibility that results might be different in older ET-patients and this should be considered in future studies. Finally, it is possible that our results are compounded by co-existent rest and physiological tremors. However, only one patient had clinically significant rest tremor and they were excluded from analyses. None of the subjects had clinically significant physiological tremor and spectral analysis indicated that the assessed tremor had a mean frequency of about 5 Hz rather than the somewhat higher frequencies associated with physiological tremor.

In summary, we provide novel evidence for the divergent roles of two key regions in ET. The emergence of peripheral tremor following the assumption of posture appears principally related to increases in tremor-frequency activity in the SMA, compared to increases in similar activity in the sensorimotor cortex in mimicked tremor in healthy controls. Furthermore, the modulation of the amplitude of established tremor by alcohol relates to changes in cerebellar activity rather than cerebral cortical areas. Taken together, these findings implicate tremor emergence as principally associated with increases in activity within frontal motor regions, whereas modulation of the amplitude of established tremor relates to changes in cerebellar activity. These findings progress a mechanistic understanding of ET and implicate network-level vulnerabilities in the rhythmic nature of communication throughout the brain.

Tables and Figures:

Table 1: General demographics for healthy control subjects and ET-patients

Figure 1: Time course of the paradigm used during the experiment. First, a short description of the upcoming task was displayed for five seconds. Then, a red cross appeared for a randomised interval of 1.3 - 4.8 secs. Turning of the red cross green signalled the instructed task (either rest condition or postural tremor/mimicked tremor). The task was ended when the green cross turned red again after a fixed 3.5 secs interval.

Figure 2: a) Mean pre-processed EMG activity of the *Musculus extensor digitorum communis* over 25 trials in one ET-patient with corresponding power spectrum for the time window of interest (1.5 - 3.5 secs). b) Effect of alcohol on tremor amplitude (log difference EMG of the EDC) for ET-patients and control group. The interrupted line at 0 illustrates no difference between the two conditions with values above indicating increase and values below decrease of tremor amplitude. Signed-rank tests demonstrated a significant increase in tremor amplitude after alcohol intake for control subjects ($*z$ = 2.20, p = .028), whereas ET-patients' tremor amplitude significantly decreased ($*z$ = -2.11, p = .035). c) Group averaged coherence for all ET-patients to illustrate corresponding results to previous literature.

Figure 3: Statistical interferences at the sensor level. a) Topographical representation of the cluster-based nonparametric permutation test in healthy control subjects with z-transformed coherence values between EEG and EDC activity at individual tremor frequencies. Significant differences between postural tremor and rest condition (upper plot) and between postural tremor and shuffled EMG (lower plot) highlighted as dark dots (both p < .01). b) The same analysis for ET-patients revealed a highly significant difference between rest and tremor conditions (p < .01 and p =.013, respectively). Sensors showing significant differences (dark dots) were located more anterior and medial compared to the healthy control group c) Averaged spectra of

the difference of z-transformed coherence (with 95% C.I.) for postural tremor versus shuffled EMG data at selected EEG sensors located over the contralateral sensorimotor cortex (sensors used are illustrated in red in the topographical representation). Spectra were offset so that peak tremor frequency was at 0 Hz across subjects, while the inset provides a histogram of individual tremor frequencies.

Figure 4: Differences in coherence (unthresholded t-statistics) between postural tremor and rest conditions at source level. a) Control subjects show significant differences between conditions (p < .01) with a spatially selective cluster demonstrating peaking at -44, -28, 60 [MNI coordinates]. Approximate locations of axial and sagittal slices are illustrated on the right as blue lines. b) In ET-patients the significant difference (p < .01) was located more medial and superior peaking at -20, -20, 68 [MNI coordinates]. Corresponding sagittal and axial slices illustrated on a coronal plane in red. Note that in a) and b) the applied ROI is outlined white whereas the clusters of significant differences are highlighted red. c) Individual coherence maxima between EMG and sources. Red circles indicate maxima for ET-patients while blue circles indicate maxima for control subjects during tremor mimicry. Multivariate Hotelling's T^2-test indicated that the maxima between groups are significantly different (χ^2= 9.8, df = 31, p < .05).

Figure 5: Effects of alcohol on postural tremor in the ET group. a) Regression maps (unthresholded t-statistics) of changes in tremor amplitude with changes in source activation. While control subjects showed no relationship between the changes in activation due to tremor in ET-patients there was a significant relationship located in the cerebellum (p = .02). This relationship could be identified across cerebellar hemispheres with a peak at -28 -84 -36 [MNI coordinates]. The applied ROI is outlined white whereas the cluster of significant relationship is highlighted red. b) Regressions of power and coherence differences (due to alcohol) for ET-patients at cerebral and cerebellar sources against the induced change in tremor amplitude. Coherence differences in the SMA were unrelated to changes in tremor amplitude following alcohol intake, whereas in the cerebellum there was a highly significant relationship. This relationship was

not due to outliers as shown using Spearman's test (ρ = .38, p = .008). There were no significant relationships with power in either the SMA or the cerebellum.

Acknowledgements

We are grateful to all of the study participants for their patience and cooperation. Furthermore, we acknowledge the work of the MR staff (Kurt Wittenberg, Antje Ruehling and Elke Bannemer) and valuable discussions with Dr. Anna Pedrosa.

Documentation of authors' roles:

David J. Pedrosa participated in the conception, organization and execution of the research project, the programming of the motor paradigms, the data assessment and data analysis, the conception and execution of the statistical analysis and the writing and critical review of the manuscript. Moreover, he had full access to all of the data in the study and takes responsibility for the integrity of the data and the accuracy of the data analysis.

Christian Nelles participated in the conception, organization and execution of the research project, the programming of the motor paradigms, the data assessment and data analysis, the conception and execution of the statistical analysis and the writing and critical review of the manuscript. Moreover, he had full access to all of the data in the study and takes responsibility for the integrity of the data and the accuracy of the data analysis.

Peter Brown participated in the data assessment and data analysis, the conception of the statistical analysis and the writing and critical review of the manuscript.

Lukas J. Volz participated in the data assessment, the data analysis, the execution of the statistical analyses and in the writing and critical review of the manuscript.

Esther A. Pelzer participated in the organization and execution of the research project, the data assessment and the critical review of the manuscript.

Marc Tittgemeyer participated in the data assessment and data analysis and in the critical review of the manuscript.

John-Stuart Brittain participated in the data assessment and data analysis, conception and execution of the statistical analysis and writing and critical review of the manuscript.

Lars Timmermann participated in the conception and organization of the research project, the data analysis and the critical review of the manuscript.

Conflict of Interest statement/Financial disclosure:

D.J.P. reports no conflicts of interest

Ch.N. reports no conflicts of interest

P.B. reports no conflicts of interest

L.J.V. reports no conflicts of interest

E.A.P. reports no conflicts of interest

M.T. reports no conflicts of interest

J.S.B. reports no conflicts of interest

L.T. received payments as a consultant for Medtronic Inc., Boston Scientific, Bayer Healthcare, UCB Schwarz Pharma. L.T. received honoraria as a speaker on symposia sponsored by TEVA Pharma, Lundbeck Pharma, Bracco, Gianni PR, Medas Pharma, UCB Schwarz Pharma, Desitin Pharma, Boehringer Ingelheim, GlaxoSmithKline, Eumecom, Orion Pharma, Medtronic Inc., Boston Scientific, Cephalon, Abott, GE Medical. The institution of L.T., not L.T. personally received funding by the German Research Foundation (DFG), the German Ministry of Education and Research, 'Manfred und Ursula Müller Stiftung', Klüh Stiftung, Hoffnungsbaum e. V., NBIA Disorders society USA, 'Köln Fortune program', Medtronic Inc., and Deutsche Parkinson Vereinigung (DPV).

D.P. is a recipient of a postdoctoral fellowship PE2291/1-1 from the Deutsche Forschungsgemeinschaft. Besides, this study was supported by the 'Köln Fortune program', the German Research Foundation (DFG, Klinische Forschergruppe KFO 219 (Ti 319/2-1)) and the Medical Research Council (MR/N003446/1 to J.S.B.).

Apart from the above, the authors report no financial conflict of interest and do not have to disclose any commercial considerations, such as an equity interest, patent rights, or

corporate affiliation, including consultantships, for any product or process mentioned in the submission.

References

Benabid, A.L., Pollak, P., Gervason, C., Hoffmann, D., Gao, D.M., Hommel, M., Perret, J.E., de Rougemont, J., 1991. Long-term suppression of tremor by chronic stimulation of the ventral intermediate thalamic nucleus. Lancet 337, 403-406.

Bhalsing, K.S., Saini, J., Pal, P.K., 2013. Understanding the pathophysiology of essential tremor through advanced neuroimaging: a review. J Neurol Sci 335, 9-13.

Boecker, H., Weindl, A., Brooks, D.J., Ceballos-Baumann, A.O., Liedtke, C., Miederer, M., Sprenger, T., Wagner, K.J., Miederer, I., 2010. GABAergic dysfunction in essential tremor: an 11C-flumazenil PET study. J Nucl Med 51, 1030-1035.

Boecker, H., Wills, A.J., Ceballos-Baumann, A., Samuel, M., Thompson, P.D., Findley, L.J., Brooks, D.J., 1996. The effect of ethanol on alcohol-responsive essential tremor: a positron emission tomography study. Ann Neurol 39, 650-658.

Brittain, J.-S., Brown, P., 2013. The many roads to tremor. Exp Neurol 250, 104-107.

Brittain, J.S., Cagnan, H., Mehta, A.R., Saifee, T.A., Edwards, M.J., Brown, P., 2015. Distinguishing the central drive to tremor in Parkinson's disease and essential tremor. J Neurosci 35, 795-806.

Broersma, M., van der Stouwe, A.M., Buijink, A.W., de Jong, B.M., Groot, P.F., Speelman, J.D., Tijssen, M.A., van Rootselaar, A.F., Maurits, N.M., 2016. Bilateral cerebellar activation in unilaterally challenged essential tremor. Neuroimage Clin 11, 1-9.

Buijink, A.W., van der Stouwe, A.M., Broersma, M., Sharifi, S., Groot, P.F., Speelman, J.D., Maurits, N.M., van Rootselaar, A.F., 2015. Motor network disruption in essential tremor: a functional and effective connectivity study. Brain 138, 2934-2947.

Cagnan, H., Brittain, J.S., Little, S., Foltynie, T., Limousin, P., Zrinzo, L., Hariz, M., Joint, C., Fitzgerald, J., Green, A.L., Aziz, T., Brown, P., 2013. Phase dependent modulation of tremor amplitude in essential tremor through thalamic stimulation. Brain 136, 3062-3075.

Ceballos-Baumann, A.O., Boecker, H., Fogel, W., Alesch, F., Bartenstein, P., Conrad, B., Diederich, N., von Falkenhayn, I., Moringlane, J.R., Schwaiger, M., Tronnier, V.M., 2001. Thalamic stimulation for essential tremor activates motor and deactivates vestibular cortex. Neurology 56, 1347-1354.

Cerasa, A., Quattrone, A., 2016. Linking Essential Tremor to the Cerebellum-Neuroimaging Evidence. Cerebellum 15, 263-275.

Craddock, M., Martinovic, J., Müller, M.M., 2015. Accounting for microsaccadic artifacts in the EEG using independent component analysis and beamforming. Psychophysiology.

Delorme, A., Sejnowski, T., Makeig, S., 2007. Enhanced detection of artifacts in EEG data using higher-order statistics and independent component analysis. Neuroimage 34, 1443-1449.

Deuschl, G., Bain, P., Brin, M., 1998. Consensus statement of the Movement Disorder Society on Tremor. Ad Hoc Scientific Committee. Mov Disord 13 Suppl 3, 2-23.

Deuschl, G., Petersen, I., Lorenz, D., Christensen, K., 2015. Tremor in the elderly: Essential and aging-related tremor. Mov Disord 30, 1327-1334.

Eickhoff, S.B., Stephan, K.E., Mohlberg, H., Grefkes, C., Fink, G.R., Amunts, K., Zilles, K., 2005. A new SPM toolbox for combining probabilistic cytoarchitectonic maps and functional imaging data. Neuroimage 25, 1325-1335.

Gallea, C., Popa, T., Garcia-Lorenzo, D., Valabregue, R., Legrand, A.P., Marais, L., Degos, B., Hubsch, C., Fernandez-Vidal, S., Bardinet, E., Roze, E., Lehericy, S., Vidailhet, M., Meunier, S., 2015. Intrinsic signature of essential tremor in the cerebello-frontal network. Brain 138, 2920-2933.

Gibson, W.S., Jo, H.J., Testini, P., Cho, S., Felmlee, J.P., Welker, K.M., Klassen, B.T., Min, H.K., Lee, K.H., 2016. Functional correlates of the therapeutic and adverse effects evoked by thalamic stimulation for essential tremor. Brain.

Gironell, A., Kulisevsky, J., Lorenzo, J., Barbanoj, M., Pascual-Sedano, B., Otermin, P., 2002. Transcranial magnetic stimulation of the cerebellum in essential tremor: a controlled study. Arch Neurol 59, 413-417.

Govindan, R.B., Raethjen, J., Arning, K., Kopper, F., Deuschl, G., 2006. Time delay and partial coherence analyses to identify cortical connectivities. Biol Cybern 94, 262-275.

Groß, J., Kujala, J., Hämäläinen, M., Timmermann, L., Schnitzler, A., Salmelin, R., 2001. Dynamic imaging of coherent sources: studying neural interactions in the human brain. Proceedings of the National Academy of Sciences 98, 694-699.

Hamalainen, M.S., Sarvas, J., 1989. Realistic conductivity geometry model of the human head for interpretation of neuromagnetic data. IEEE Trans Biomed Eng 36, 165-171.

Haslinger, B., Boecker, H., Buchel, C., Vesper, J., Tronnier, V.M., Pfister, R., Alesch, F., Moringlane, J.R., Krauss, J.K., Conrad, B., Schwaiger, M., Ceballos-Baumann, A.O., 2003. Differential modulation of subcortical target and cortex during deep brain stimulation. Neuroimage 18, 517-524.

Hellriegel, H., Schulz, E.M., Siebner, H.R., Deuschl, G., Raethjen, J.H., 2012. Continuous theta-burst stimulation of the primary motor cortex in essential tremor. Clin Neurophysiol 123, 1010-1015.

Hellwig, B., Haussler, S., Schelter, B., Lauk, M., Guschlbauer, B., Timmer, J., Lucking, C.H., 2001. Tremor-correlated cortical activity in essential tremor. Lancet 357, 519-523.

Helmich, R.C., Janssen, M.J., Oyen, W.J., Bloem, B.R., Toni, I., 2011. Pallidal dysfunction drives a cerebellothalamic circuit into Parkinson tremor. Ann Neurol 69, 269-281.

Hotelling, H., 1931. The Generalization of Student's Ratio. The Annals of Mathematical Statistics 2, 360-378.

Jenkins, I.H., Bain, P.G., Colebatch, J.G., Thompson, P.D., Findley, L.J., Frackowiak, R.S., Marsden, C.D., Brooks, D.J., 1993. A positron emission tomography study of essential tremor: evidence for overactivity of cerebellar connections. Ann Neurol 34, 82-90.

Kalbe, E., Kessler, J., Calabrese, P., Smith, R., Passmore, A.P., Brand, M., Bullock, R., 2004. DemTect: a new, sensitive cognitive screening test to support the diagnosis of mild cognitive impairment and early dementia. Int J Geriatr Psychiatry 19, 136-143.

Kelly, R.M., Strick, P.L., 2003. Cerebellar loops with motor cortex and prefrontal cortex of a nonhuman primate. J Neurosci 23, 8432-8444.

Klein, J.C., Barbe, M.T., Seifried, C., Baudrexel, S., Runge, M., Maarouf, M., Gasser, T., Hattingen, E., Liebig, T., Deichmann, R., Timmermann, L., Weise, L., Hilker, R., 2012. The tremor network targeted by successful VIM deep brain stimulation in humans. Neurology 78, 787-795.

Lu, M.K., Chiou, S.M., Ziemann, U., Huang, H.C., Yang, Y.W., Tsai, C.H., 2015. Resetting tremor by single and paired transcranial magnetic stimulation in Parkinson's disease and essential tremor. Clin Neurophysiol 126, 2330-2336.

Maris, E., 2012. Statistical testing in electrophysiological studies. Psychophysiology 49, 549-565.

Maris, E., Oostenveld, R., 2007. Nonparametric statistical testing of EEG- and MEG-data. J Neurosci Methods 164, 177-190.

Marsden, J.F., Ashby, P., Limousin-Dowsey, P., Rothwell, J.C., Brown, P., 2000. Coherence between cerebellar thalamus, cortex and muscle in man: cerebellar thalamus interactions. Brain 123 (Pt 7), 1459-1470.

McIntyre, C.C., Savasta, M., Kerkerian-Le Goff, L., Vitek, J.L., 2004a. Uncovering the mechanism(s) of action of deep brain stimulation: activation, inhibition, or both. Clin Neurophysiol 115, 1239-1248.

McIntyre, C.C., Savasta, M., Walter, B.L., Vitek, J.L., 2004b. How does deep brain stimulation work? Present understanding and future questions. J Clin Neurophysiol 21, 40-50.

Middleton, F.A., Strick, P.L., 2001. Cerebellar projections to the prefrontal cortex of the primate. J Neurosci 21, 700-712.

Mitra, P.P., Pesaran, B., 1999. Analysis of dynamic brain imaging data. Biophys J 76, 691-708.

Mooney, C.Z., Duval, R.D., Duval, R., 1993. Bootstrapping: A nonparametric approach to statistical inference. Sage.

Muthuraman, M., Hellriegel, H., Hoogenboom, N., Anwar, A.R., Mideksa, K.G., Krause, H., Schnitzler, A., Deuschl, G., Raethjen, J., 2014. Beamformer source analysis and connectivity on concurrent EEG and MEG data during voluntary movements. PLoS One 9, e91441.

Muthuraman, M., Heute, U., Arning, K., Anwar, A.R., Elble, R., Deuschl, G., Raethjen, J., 2012. Oscillating central motor networks in pathological tremors and voluntary movements. What makes the difference? Neuroimage 60, 1331-1339.

Neely, K.A., Kurani, A.S., Shukla, P., Planetta, P.J., Wagle Shukla, A., Goldman, J.G., Corcos, D.M., Okun, M.S., Vaillancourt, D.E., 2015. Functional Brain Activity Relates to 0-3 and 3-8 Hz Force Oscillations in Essential Tremor. Cereb Cortex 25, 4191-4202.

Negro, F., Keenan, K., Farina, D., 2015. Power spectrum of the rectified EMG: when and why is rectification beneficial for identifying neural connectivity? J Neural Eng 12, 036008.

Okada, Y., Lauritzen, M., Nicholson, C., 1987. MEG source models and physiology. Physics in medicine and biology 32, 43.

Pedrosa, D.J., Quatuor, E.L., Reck, C., Pauls, K.A., Huber, C.A., Visser-Vandewalle, V., Timmermann, L., 2014. Thalamomuscular coherence in essential tremor: hen or egg in the emergence of tremor? J Neurosci 34, 14475-14483.

Pedrosa, D.J., Reck, C., Florin, E., Pauls, K.A., Maarouf, M., Wojtecki, L., Dafsari, H.S., Sturm, V., Schnitzler, A., Fink, G.R., Timmermann, L., 2012. Essential tremor and tremor in Parkinson's disease are associated with distinct 'tremor clusters' in the ventral thalamus. Exp Neurol 237, 435-443.

Perlmutter, J.S., Mink, J.W., Bastian, A.J., Zackowski, K., Hershey, T., Miyawaki, E., Koller, W., Videen, T.O., 2002. Blood flow responses to deep brain stimulation of thalamus. Neurology 58, 1388-1394.

Perrin, F., Pernier, J., Bertrand, O., Echallier, J.F., 1989. Spherical splines for scalp potential and current density mapping. Electroencephalogr Clin Neurophysiol 72, 184-187.

Phillips, C., 2000. Source estimation in EEG: Combining anatomical and functional constraints. PhD Thesis.

Pinto, A.D., Lang, A.E., Chen, R., 2003. The cerebellothalamocortical pathway in essential tremor. Neurology 60, 1985-1987.

Popa, T., Russo, M., Vidailhet, M., Roze, E., Lehericy, S., Bonnet, C., Apartis, E., Legrand, A.P., Marais, L., Meunier, S., Gallea, C., 2013. Cerebellar rTMS stimulation may induce prolonged clinical benefits in essential tremor, and subjacent changes in functional connectivity: an open label trial. Brain Stimul 6, 175-179.

Raethjen, J., Deuschl, G., 2012. The oscillating central network of Essential tremor. Clin Neurophysiol 123, 61-64.

Raethjen, J., Govindan, R.B., Kopper, F., Muthuraman, M., Deuschl, G., 2007. Cortical involvement in the generation of essential tremor. J Neurophysiol 97, 3219-3228.

Schnitzler, A., Munks, C., Butz, M., Timmermann, L., Gross, J., 2009. Synchronized brain network associated with essential tremor as revealed by magnetoencephalography. Mov Disord 24, 1629-1635.

Schoffelen, J.M., Gross, J., 2009. Source connectivity analysis with MEG and EEG. Hum Brain Mapp 30, 1857-1865.

Taha, J.M., Janszen, M.A., Favre, J., 1999. Thalamic deep brain stimulation for the treatment of head, voice, and bilateral limb tremor. J Neurosurg 91, 68-72.

Thomson, D.J., 1982. Spectrum estimation and harmonic analysis. Proceedings of the IEEE 70, 1055-1096.

Tzourio-Mazoyer, N., Landeau, B., Papathanassiou, D., Crivello, F., Etard, O., Delcroix, N., Mazoyer, B., Joliot, M., 2002. Automated anatomical labeling of activations in SPM using a macroscopic anatomical parcellation of the MNI MRI single-subject brain. Neuroimage 15, 273-289.

Wills, A.J., Jenkins, I.H., Thompson, P.D., Findley, L.J., Brooks, D.J., 1994. Red nuclear and cerebellar but no olivary activation associated with essential tremor: a positron emission tomographic study. Ann Neurol 36, 636-642.

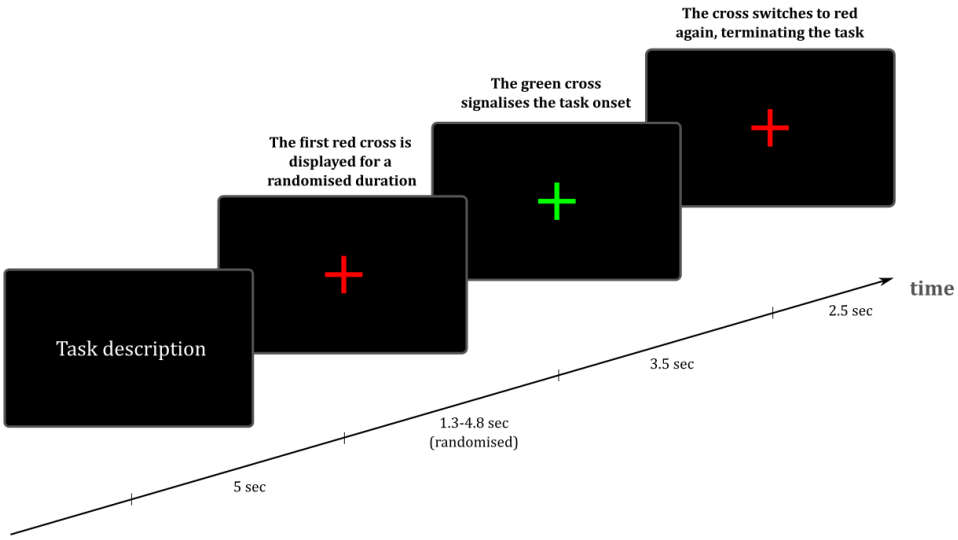

Fig. 1

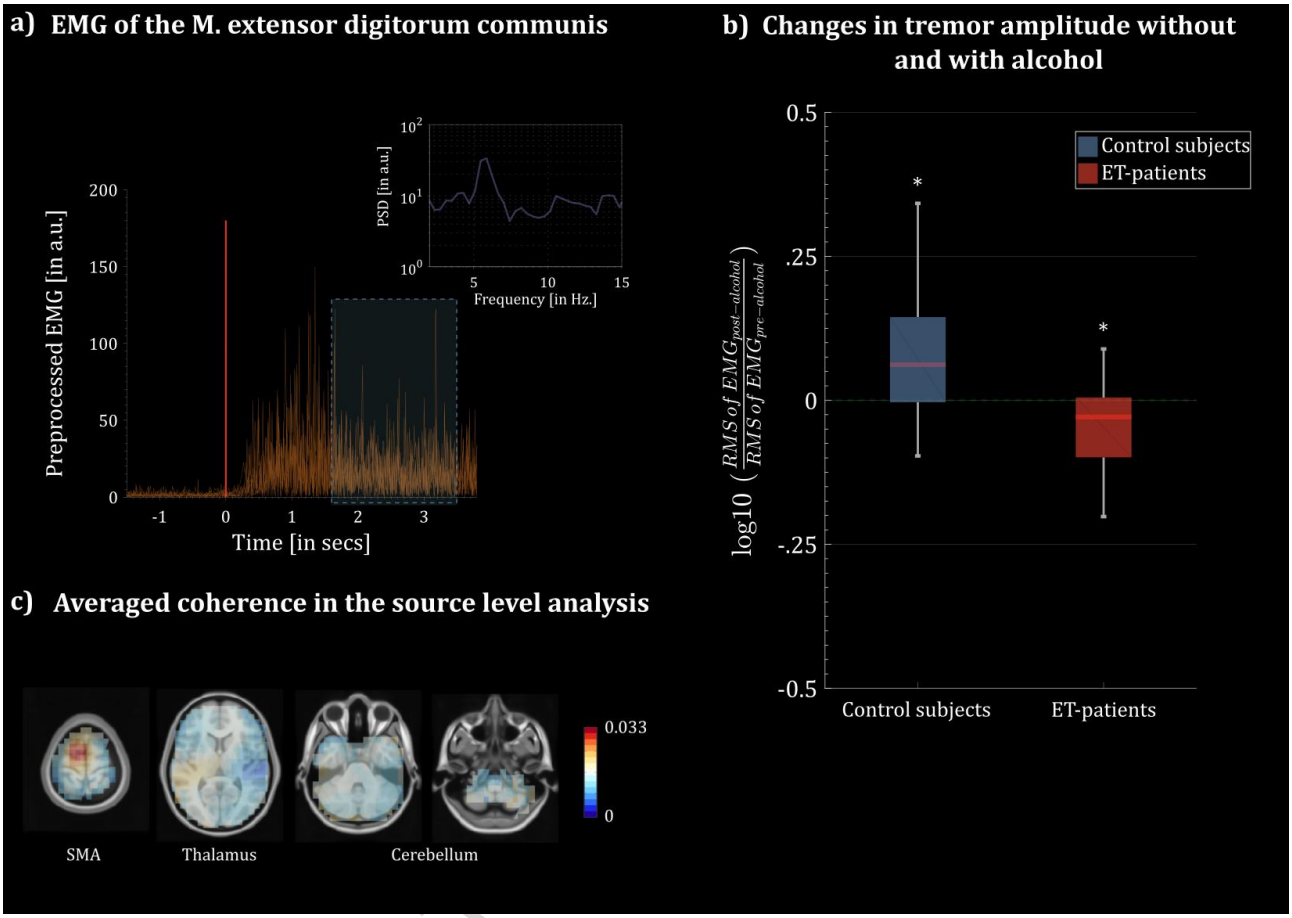

Fig. 2

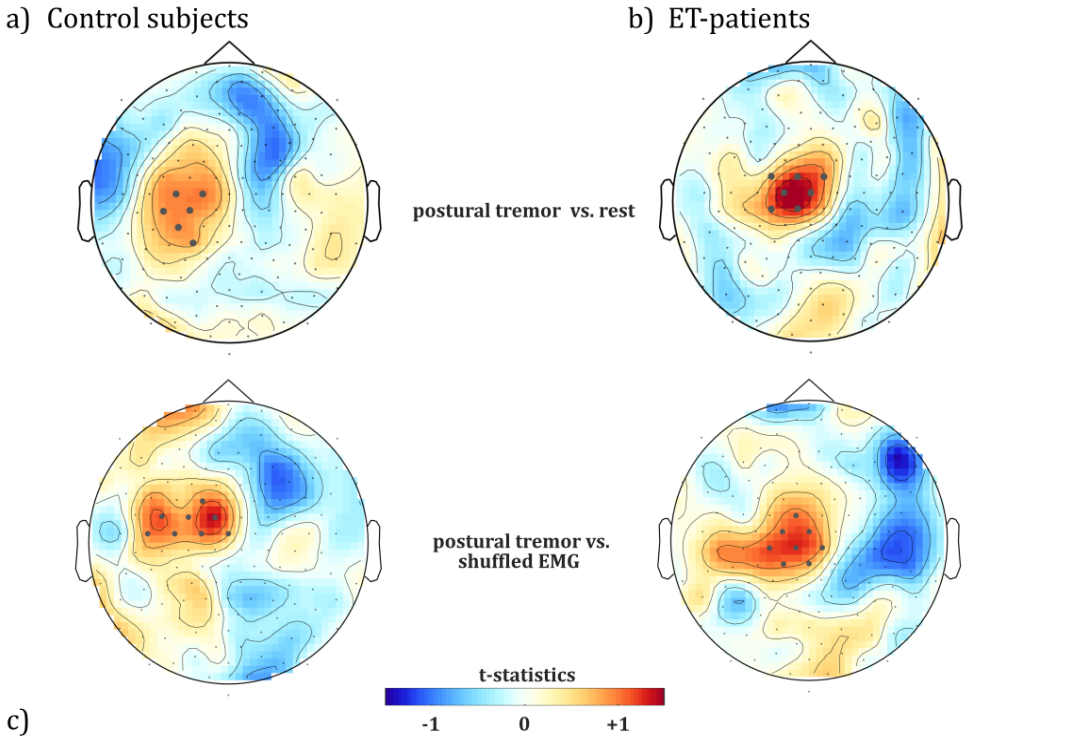

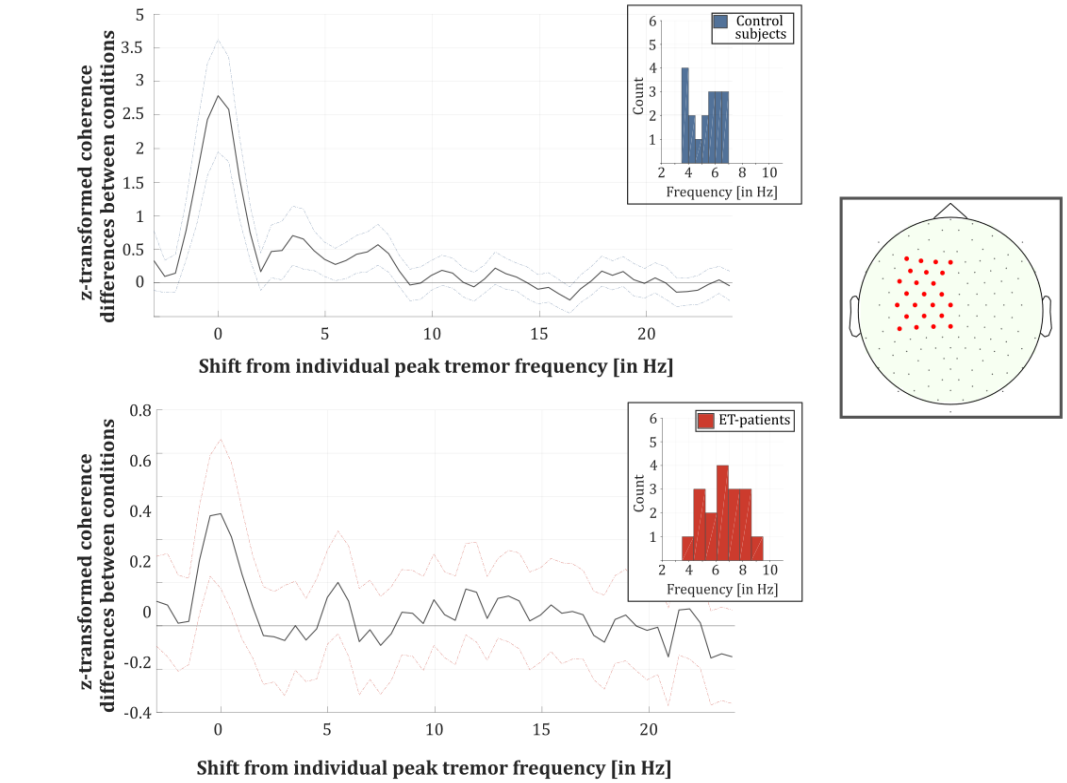

Fig. 3

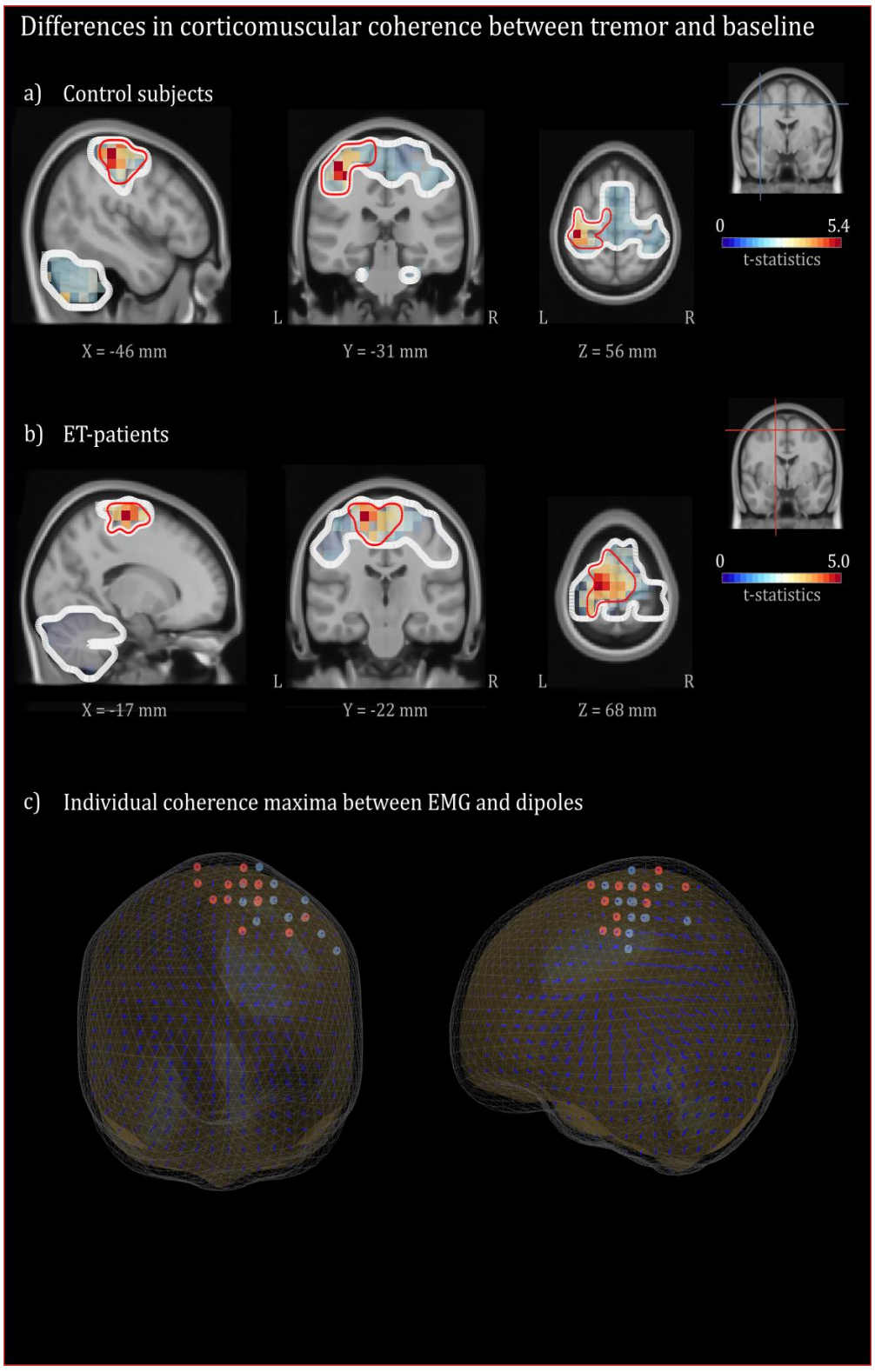

Fig. 4

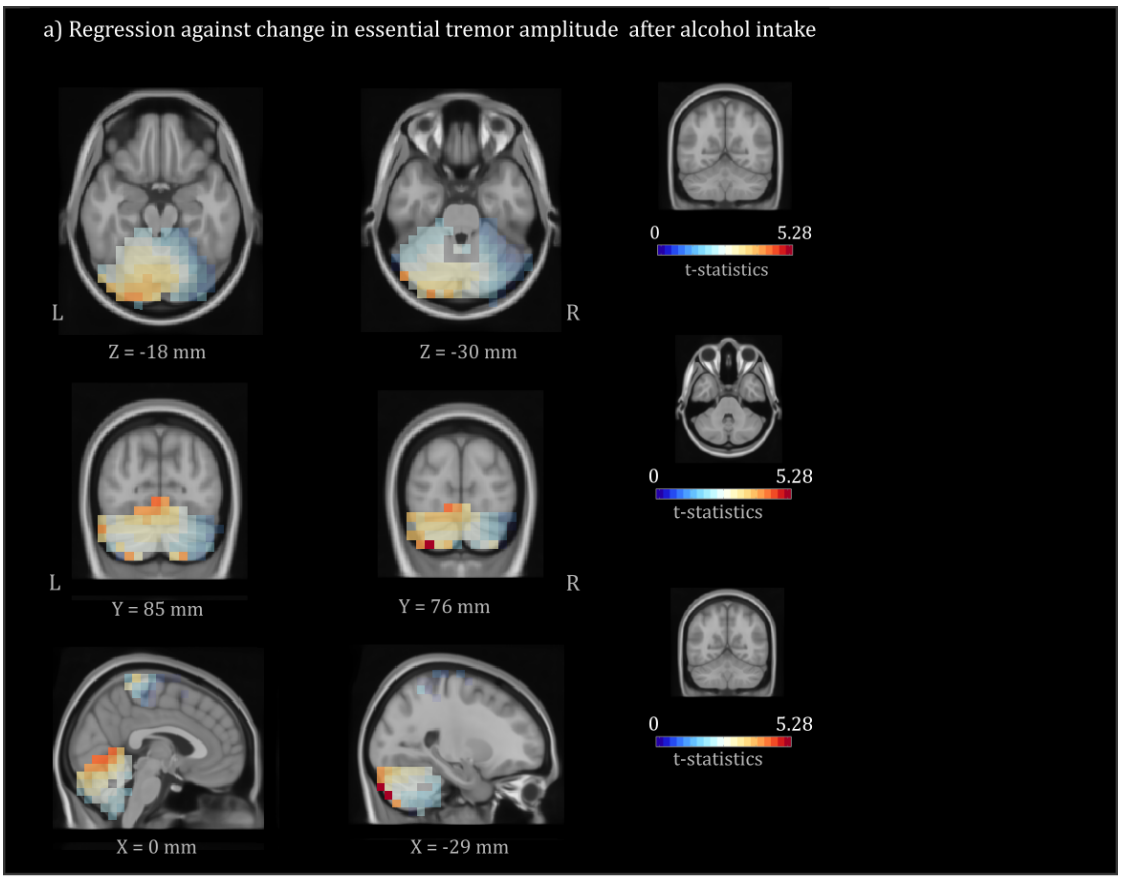

b) Regressions between differences in power and coherence with tremor amplitude changes for ET-patients

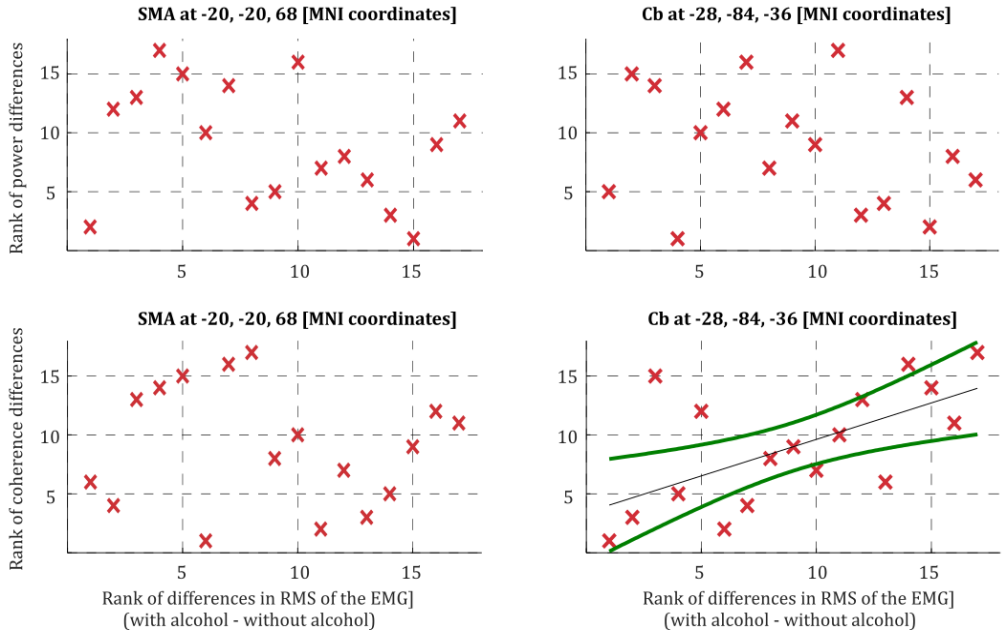

Fig. 5

Table 1: General demographics for healthy control subjects and ET-patients

	ET-patients (n =17)	Control subjects (n = 18)	p-value[a]
Age [in years]	51.1 ± 14.5	48.6 ± 17.9	$p = .661$
Gender (female vs. male)	8:9	10:8	-
Disease duration [in years]	26.2 ± 15.3	n.a.	-
Response time [in msec.]	234.8 ± 52.9	238.3 ± 50.1	$p = .841$
RMS tremor amplitude without alcohol [in a.u.]	16.9 ± 12.8	36.0 ± 19.3	$p < .001$[b,c]
RMS tremor amplitude with alcohol [in a.u.]	15.2 ± 10.9	43.0 ± 22.2	$p < .001$[b,c]

[a] if not indicated specifically, differences between conditions resulted from paired samples t-tests (level of significance $\alpha = .05$) when Kolmogorov-Smirnov test indicated normal distribution

[b] tested using a Wilcoxon Mann Whitney test.

[c] within-group differences between RMS with and without alcohol are illustrated in Figure 2.

Highlights

Cortical involvement in ET diverges spatially from the one throughout mimicked tremor

Alcohol effects revealed segregated networks underlying ET onset and its subsistence

Our data emphasize the idea of cortical involvement gating cerebellar dysfunction